Environmental Science & Technology

pubs.acs.org/est

Article

Deregulation of Ribosome Biogenesis in Nitrite-Oxidizing Bacteria Leads to Nitrite Accumulation

Weiping Xiong, Yuhang Ye, Dandan He, Siying He, Yinping Xiang, Jun Xiao, Wenyi Feng, Mengru Wu, Zhaohui Yang, and Dongbo Wang*

Cite This: https://doi.org/10.1021/acs.est.3c06002

Read Online

ACCESS | Metrics & More | Article Recommendations | Supporting Information

ABSTRACT: Nitrite (NO_2^-) accumulation caused by nitrite-oxidizing bacteria (NOB) inhibition in nitrification is a double-edged sword, i.e., a disaster in aquatic environments but a hope for innovating nitrogen removal technology in wastewater treatment. However, little information is available regarding the molecular mechanism of NOB inhibition at the cellular level. Herein, we investigate the response of NOB inhibition on NO_2^- accumulation established by a side-stream free ammonia treatment unit in a nitrifying reactor using integrated metagenomics and metaproteomics. Results showed that compared with the baseline, the relative abundance and activity of NOB in the experimental stage decreased by 91.64 and 68.66%, respectively, directly resulting in a NO_2^- accumulation rate of 88%. Moreover, RNA polymerase, translation factors, and aa-tRNA ligase were significantly downregulated, indicating that protein synthesis in NOB was interfered during NO_2^- accumulation. Further investigations showed that ribosomal proteins and GTPases, responsible for bindings between either ribosomal proteins and rRNA or ribosome subunits, were remarkably downregulated. This suggests that ribosome biogenesis was severely disrupted, which might be the key reason for the inhibited protein synthesis. Our findings fill a knowledge gap regarding the underlying mechanisms of NO_2^- accumulation, which would be beneficial for regulating the accumulation of NO_2^- in aquatic environments and engineered systems.

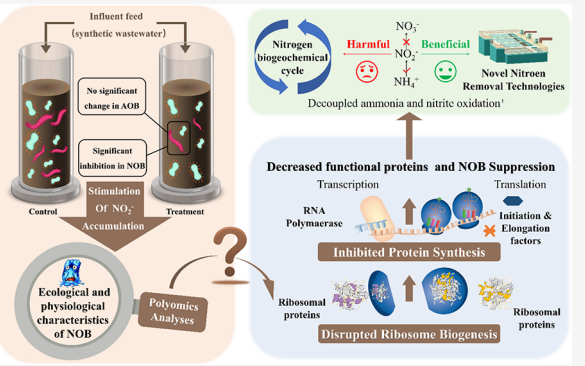

KEYWORDS: *nitrite-oxidizing bacteria, nitrite accumulation, polyomics, ribosome, protein synthesis*

INTRODUCTION

Nitrification mediated by microbes is the only oxidation reaction linking the reduced (ammonium, NH_4^+) and oxidized (nitrite, NO_2^- and nitrate, NO_3^-) inorganic nitrogen pools in the global nitrogen cycle. Specifically, nitrification is a two-step process accomplished by distinctly different nitrifiers.[1] NH_4^+ is oxidized to NO_2^- by ammonia-oxidizing bacteria (AOB) (sometimes ammonia-oxidizing archaea, AOA and complete ammonia oxidizer, comammox) and then further converted to NO_3^- by nitrite-oxidizing bacteria (NOB). Theoretically, NO_2^- rarely accumulates in complete nitrification, as there is thought to be a high mutual benefit between AOB and NOB. They usually work in concert, which is the basis of the global nitrogen cycle.[2,3] However, the accumulation of NO_2^- has been widely reported in aquatic and engineered water systems. For example, Schaefer and Hollibaugh observed that NO_2^- concentrations can exceed 10 μM during summer in estuarine waters adjacent to Sapelo Island in U.S.A.[4] Nevertheless, restricting ammonia oxidation to nitrite instead of nitrate has been proposed as a promising novel nitrogen removal approach for wastewater treatment. Nitrification terminated at nitrite followed by denitrification or anaerobic ammonium oxidation (anammox) could reduce 25% of aeration consumption,[5] 40% for denitrification, and nearly 100% for anammox of the carbon source demand,[5,6] which have attracted ongoing attention recently as such impressive benefits.

For better regulation of NO_2^- accumulation, numerous studies were conducted to investigate the causes of NO_2^- accumulation in both aquatic environments and engineered systems. The instability of the NOB is considered one of the main reasons for the induction of NO_2^- accumulation. NOB is considered the most unstable among guilds and exhibits a different general pattern of instability in nitrification.[7] In particular, the review of Sarah et al. concluded that the accumulation of NO_2^- was directly caused by the loss of nitrite oxidation capacity due to the inhibition of NOB.[8] Taking the

Received: July 26, 2023
Revised: September 28, 2023
Accepted: October 6, 2023

typical biocide free ammonia (FA) as an example, NOB activity (i.e., nitrite oxidation capacity) was inhibited by more than 50% under the stress of an FA concentration of 0.7 mg NH_3−N/L.[9] However, further investigations did not explain exactly how the NOB inhibition occurs. Vadivelu et al.[10] proposed that FA inhibits the anabolic processes of NOB *Nitrobacter,* thus stopping the growth of NOB and causing NO_2^- accumulation. At the same time, Sun et al. reported that though the abundance of *nxrA* and *nxrB* genes remained stable, the abundance and activity of NOB decreased significantly under FA stress.[11] Previous studies explored the possible reasons for NOB inhibition from different perspectives such as nitrification kinetics, community composition, and gene relative abundance but failed to clarify what intracellular changes occur that lead to NOB inhibition and ultimately cause the loss of nitrite-oxidizing capacity. In aquatic environments, even sporadic accumulation of NO_2^- can pose serious environmental risks. The potential ecosystem consequences of NO_2^- accumulation include increased N_2O production[12] and toxicity to a suite of aquatic organisms.[13] In engineered systems, however, stable NOB suppression is highly expected but remains a big challenge. The phylogenetic and physiological diversities of NOB that result in the difficulty in stable NOB suppression were reported recently, but little is known regarding the key physiological features for achieving stable NOB suppression. Revealing the fundamental mechanisms of NO_2^- accumulation would help to develop effective methods for improving the solution of natural environmental hazards and the development of novel nitrogen removal technologies.

It is generally acknowledged that the essence of NO_2^- oxidation is an enzyme-catalyzed process driven by nitrite oxidoreductase (NXR, NO_2^- to NO_3^-), which is essentially a protein. In addition, various other proteins are required for NOB growth. These enzymes (proteins) come from a complex enzyme (protein) synthesis process from genes to proteins, i.e., genetic central dogma. In short, DNA is first transcribed into mRNA, after which mRNA is used as a template to synthesize proteins in translation.[14,15] In addition, the enzyme (protein) synthesis is done by multimolecular factories called ribosomes, which makes ribosomes lie at the core of cell growth.[16] According to the previous literature, there was no significant change in gene abundance of NXR during NO_2^- accumulation,[11] but no activity of NXR was detected (i.e., there was no nitrite oxidation). It is therefore assumed that NO_2^- accumulation may be caused by the deregulation of enzyme (protein) synthesis or ribosome. However, the limited gene-centered information from previous studies could not shed light on this perspective. Metaproteomic can annotate large-scale proteins for information about specific enzymes and assign them to specific microbial species, which is good for understanding the enzyme (protein) synthesis process involving many functional proteins (e.g., transcription enzymes and translation factors) and ribosome consisting of ribosomal proteins. Therefore, the regulation of ribosome and enzyme (protein)synthesis of NOB can be deeply elucidated by applying metaproteomic based on metagenomic.

In this study, two lab-scale reactors (namely, control and treatment reactors) were operated to enrich nitrifiers and establish NO_2^- accumulation. Sludge treatment using biocide FA exerted by a side-stream line was chosen as the typical method to achieve NO_2^- accumulation. FA is the un-ionized form of ammonium, which inevitably occurs under alkaline conditions with high concentrations of ammonium in both aquatic environments and engineered systems.[17,18] Then, label-free metaproteomics based on metagenomics were used to investigate the microscopic changes in enzyme synthesis processes of NOB causing the accumulation of NO_2^-. Our results fill a knowledge gap on the microscopic response mechanisms of NOB during NO_2^- accumulation, which not only provides valuable insights into the regulations of NO_2^- accumulation in aquatic environments but also facilitates the improvement of novel nitrogen removal technology.

MATERIAL AND METHODS

Reactor Operation, Monitoring, and Sample Collection. The inoculated sludge, which was taken from a wastewater treatment plant (WWTP) in Changsha, China, was seeded to operate two 4 L reactors supplied with synthetic wastewater (please see composition below) without organic carbon sources to enrich nitrifiers.[19] One was set as the control, and the other was set as the treatment reactor. The reactors were continuously operated for over 200 days in a temperature-controlled laboratory (21−23 °C), consisting of the baseline and experimental stages. The initial baseline stage (days 0−110) was designed to enhance the growth of nitrifiers. The reactors were operated with a cycle daily in the baseline stage. Each cycle lasted 24 h, comprising a 5 min feeding stage (feeding 1.5 L of synthetic wastewater), a 9 h aerobic mixing period, a 50 min settling stage, a 5 min drainage period, and a 14 h idle period.

In the experimental stage (day 110−210), the two reactors were operated with two cycles. Each cycle lasted 12 h, comprising a 5 min feeding stage (feeding 1.5 L of synthetic wastewater), a 9 h aerobic mixing period, a 50 min settling stage, a 5 min drainage period, and a 2 h idle period. In this stage, FA-based side-stream treatment was implemented in the treatment reactor. In short, 500 mL of the mixture was extracted from the main reactor at the end of each aerobic mixing period for the side-stream treatment. After the mixture was thickened to 100 mL, it was treated for 24 h with a concentration of 500 mg NH_3−N/L at pH 8.9 (leading an FA concentration of 130 mg NH_3−N/L). Then, the sludge was rinsed with deionized water until ammonia was completely washed out and then recirculated back to the main reactor. The side-stream treatment was proposed as an effective way to establish NO_2^- accumulation in previous study,[20] thus ensuring that NOB would be inhibited, but not inactivated entirely and sufficient protein samples from NOB (measured by BCA method) could be collected and analyzed.

During the whole experiment, dissolved oxygen concentration of 2.5−3 mg/L and pH value of 7.5−7.7 were regulated by programmed logic controllers in the aeration period. Since synthetic wastewater does not contain organic carbon sources, there is no sludge waste sludge except loss via effluent. The reactors were operated continuously until the effluent NH_4^+, NO_2^-, and NO_3^- concentrations and AOB and NOB activities reached stability. The determinations of NH_4^+, NO_2^-, and NO_3^- were carried out by standard methods (three times a week), and the activities of nitrifiers were determined by batch experiments (Supporting Information). Once the reactors reached stability, triplicate samples were systematically collected over three consecutive days from each reactor for metagenomic and metaproteomic analyses (three samples in total for each reactor). The three consecutively collected

https://doi.org/10.1021/acs.est.3c06002
Environ. Sci. Technol. XXXX, XXX, XXX−XXX

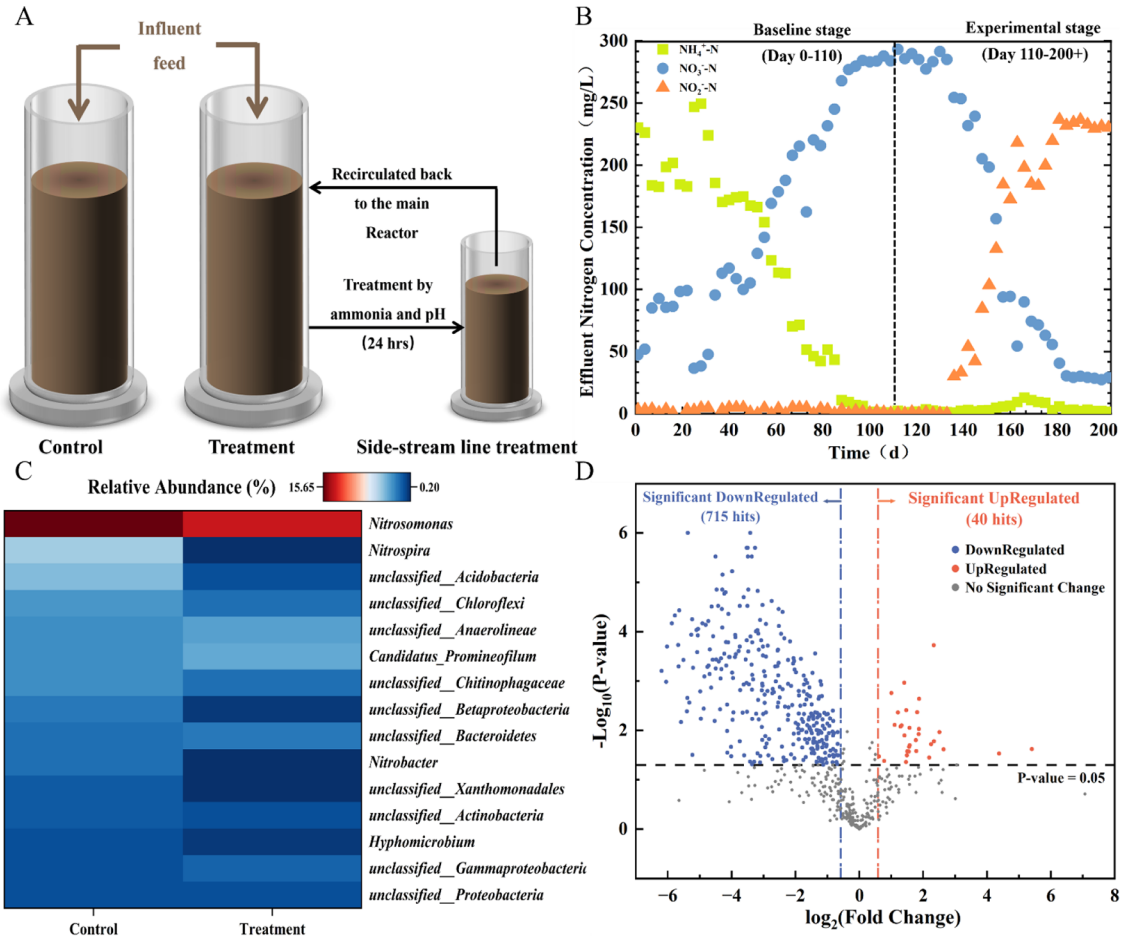

Figure 1. (A) Schematic diagram of two reactors in the experimental stage. (B) Effluent ammonium, nitrite, and nitrate levels in the treatment reactor. (C) Top 15 genera of microbial community detected in the control and treatment reactors in 200 days. (D) The volcano plot shows the number of differentially expressed proteins (treatment to control) for samples which triplicate meet the stringency levels of p-value ≤0.05, setting the foldchange thresholds as follows: foldchange > 1.5, upregulated (orange); foldchange < 0.6, downregulated (blue).

samples from each reactor were considered to be parallel and grouped together for subsequent analysis.

Composition of Synthetic Wastewater. Each liter of synthetic wastewater consists of 1150 mg of NH_4Cl (equivalent to 300 mg of NH_3−N/L), 13 mg of K_2HPO_4, 14 mg of KH_2PO_4, 1000 mg of $NaHCO_3$, 5 mg of $CaCl_2$, 10 mg of $MgCl_2$, and 0.5 mL of trace element solution. Each liter of trace element solution consists of 1.5 g of $FeCl_3{\cdot}6H_2O$, 0.12 g of $ZnSO_4{\cdot}7H_2O$, 0.06 g of $Na_2MoO_4{\cdot}2H_2O$, 0.15 g of H_3BO_3, 0.03 g of $CuSO_4{\cdot}5H_2O$, 0.18 g of KI, 0.12 g of $MnCl_2{\cdot}4H_2O$, 0.15 g of $CoCl_2{\cdot}6H_2O$, and 10 g of EDTA.[21]

Metagenomic Analysis. For metagenomic analysis, DNA extraction was exerted first, as detailed in the Supporting Information. For subsequent analysis, a total of 153123014 raw reads (PE150, 150 bp paired end reads) from the sample were processed to remove low-quality reads as follows. The fastp software (https://github.com/OpenGene/fastp) was applied to eliminate the adapter sequences from the 5′ end and 3′ end. After that, low-quality reads (shorter than 50 bp, containing N bases, or with a mean quality below 20) were removed by the library sickle (https://github.com/najoshi/sickle). The coverage of the filtered 150720472 reads was between 98.3 and 98.5% with a reliable accuracy (Table S1). Furthermore, the filtered clean reads from all samples underwent assembly using MEGAHIT (v1.1.3) with default parameters.[22] For gene prediction and taxonomy annotation, open reading frames (ORFs) were predicted by searching the assembled contigs (≥300 bp in length) using MetaGene (http://metagene.cb.k.u-tokyo.ac.jp/).[23] The predicted ORFs (≥100 bp in length) were retrieved and translated into amino acid sequences by the National Center for Biotechnology Information (NCBI) translation table. All predicted ORFs were subjected to clustering at 95% sequence identity and 90% coverage by CD-HIT (http://www.bioinformatics.org/cd-hit/)[24] to construct a nonredundant gene catalog. After quality control, the reads were aligned to the representative sequences with a 95% identity threshold using SOAPaligner (http://soap.genomics.org.cn/),[25] and gene abundance in each sample was evaluated. Representative sequences of the nonredundant gene catalog were aligned to NCBI NR database for taxonomic annotations with an e-value cutoff of $1e^{-5}$ using BLASTP (Version 2.2.28+, http://blast.ncbi.nlm.nih.gov/Blast.cgi).

Metaproteomic Analysis. For metaproteomic analysis, protein extraction was first carried out followed by protein dissolution and then the high-performance liquid chromatography (HPLC) assay and mass spectrometry analysis. Descriptions of protein extraction and dissolution, the high-performance liquid chromatography (HPLC) assay, and mass spectrometry analysis were conducted and detailed in the Supporting Information. For sequence database searching, MS/MS spectra were searched by Proteome Discoverer TM Software 2.4 software against the translated metagenomic

https://doi.org/10.1021/acs.est.3c06002
Environ. Sci. Technol. XXXX, XXX, XXX−XXX

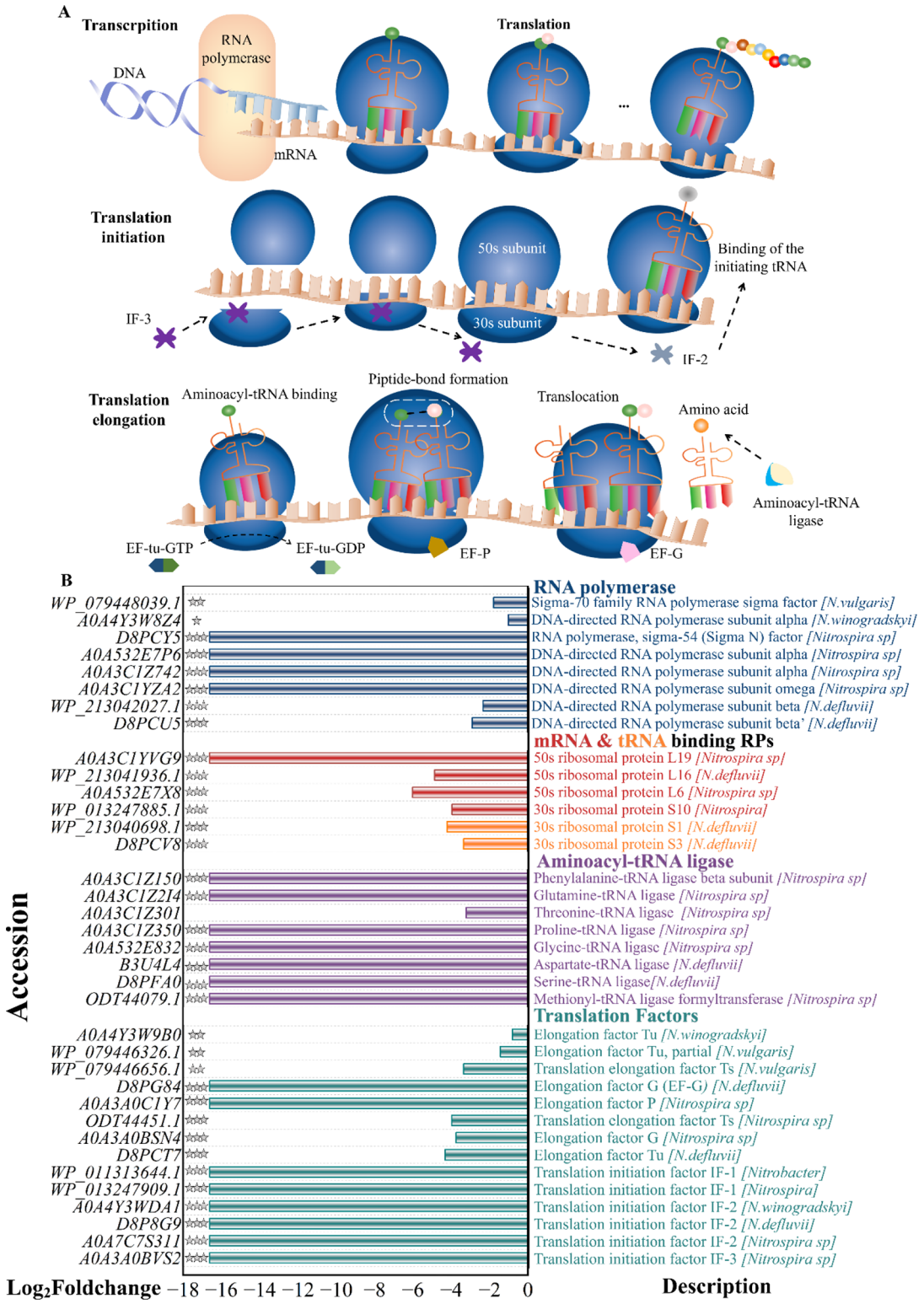

Figure 2. (A) Schematic representation of the roles of RNA polymerase and translation factors in protein synthesis, showing mainly the inhibited processes, i.e., transcription, initiation, and elongation of translation. (B) Regulation of the significantly downregulated vital proteins, including RNA polymerase, ribosomal proteins involved in binding with mRNA or tRNA, translation factors, and aa-tRNA ligase; one pentagram represents significant ($P \leq 0.05$), two are highly significant ($P \leq 0.01$), and three are extremely significant ($P \leq 0.001$).

database, as well as public databases such as Uniprot and NCBI. To ascertain parent proteins, the highest score for a given peptide mass indicating the best match predicted in the database was used. The parameters for protein searching were configured with the following settings: tryptic digestion allowing for up to two missed cleavages, carbamidomethylation of cysteines as a static modification, and dynamic modifications, including oxidation of methionines and protein N-terminal acetylation. Validation of peptide spectral matches was conducted based on *q*-values at a false discovery rate of

https://doi.org/10.1021/acs.est.3c06002
Environ. Sci. Technol. XXXX, XXX, XXX−XXX

1%. For differential expression analysis, specifically, a protein that met a p-value stringency of ≤0.05 in triplicate was considered significantly changed in expression, a p-value of ≤0.01 was considered highly significant, and a p-value of ≤0.001 was considered extremely significant (setting the upregulated foldchange (FC) at 1.5 and the downregulated at 0.6). It is important to note that the proteins we discussed in the latter section are all differentially expressed proteins (DEPs) with statistical significance. Foldchange, $\log_2$FC and p-values for all DEPs are provided in Table S1. The taxonomic classification involved comparing the protein sequences with the NR database, while the functional annotation of all identified proteins was performed using the Kyoto Encyclopedia of Genes and Genomes (KEGG) pathway database (http://www.genome.jp/kegg/). The metagenomic sequence data have been submitted to the NCBI with the accession number PRJNA901239. Likewise, the metaproteomic data have been deposited in the ProteomeXchange Consortium and can be accessed with the data set identifier PXD041274.

RESULTS AND DISCUSSION

Performance and Microbial Community Composition of the Reactors. As the baseline stage of the experiment progressed, the NH_4^+−N concentration in the effluent maintained a steady decreasing trend while the NO_3^- concentration increased steadily (Figure 1B), indicating that the nitrifiers were gradually enriched. At the end of the baseline stage, near-thorough conversion of NH_4^+ to NO_3^- occurred (Figure 1B and Figure S2) in both reactors (control and treatment), indicating the high activity of nitrifiers. Though a brief nitrite peak was observed during each cycle, nitrite was eventually converted to nitrate (Figure S5). Following the baseline stage, the experimental stage (days 110−200) commenced with (Figure 1A). No significant change in the effluent was observed during the first 20 days of the experimental stage (day 110−130), after which accumulation of NO_2^- occurred. At the end of the experimental stage, NH_4^+ in the Treatment Reactor was nearly completely converted to a mixture of NO_2^- (88.02 ± 0.37% of the total effluent nitrogen) and NO_3^- (11.04 ± 0.28% of the total effluent nitrogen) (Figure 1B).

The obvious NO_2^- accumulation, which means loss of nitrite oxidation capacity, may be explained by two aspects. On the one hand, the relative abundance of NOB sharply reduced in the treatment reactor. Specifically, the dominant NOB genus *Nitrospira* and *Nitrobacter* represented 5.42 and 2.24% of the microbial communities in the control reactor, respectively, and reduced to 0.21 and 0.43% in the treatment reactor (Figure 1C). It is noteworthy that the abundance of denitrifiers, such as *Comamonas* and *Sphingopyxis*, significantly increased (Figure S4). Previous studies reported that FA may kill some microorganisms such as NOB, making them potential source of organic carbon for denitrification. On the other hand, NOB activity, indicated by nitrite oxidation rate, decreased from 53.73 ± 1.73 mg N/g VSS h to 16.84 ± 3.69 mg N/g VSS h in the treatment reactor (Table S3). Thus, it can be understood that the NOB was inhibited and gradually eliminated, which directly caused NO_2^- accumulation.

Further, results from the metaproteomic analysis showed that 755 DEPs were detected within NOB, and 715 DEPs were detected as downregulated (FC < 0.6), while only 40 of them were upregulated (Figure. 1D). The downregulation of these DEPs could explain the inhibition of NOB and the accumulation of NO_2^- to some extent. Notably, the key enzyme of NOB (i.e., NXR) that catalyzes the conversion of NO_2^- to NO_3^- and shuttles two electrons in each reaction as an energy source to sustain life activities,[26] was detected to be downregulated significantly. This was consistent with the observed decrease in nitrite oxidation capacity (53.734 ± 1.73 to 16.849 ± 3.69 mg N/g VSS h) (Table S3), indicating that NOB may fail to oxidize nitrite to maintain activity and cause NO_2^- accumulation. Therefore, it is worth considering the underlying reasons for the decrease in these critical enzymes (proteins). Similar to the results reported by Sun et al.,[11] the results from metagenomic showed that the relative abundance of nxrA and nxrB did not decrease as strongly as the abundance and activity of NOB. The relative abundance of nxrA (7.92 to 5.306%) and nxrB (4.33 to 3.152%) decreased by 33.02 and 31.73%, respectively, while the relative abundance and activity of NOB decreased by 91.64 and 68.66%, respectively. A plausible speculation was that the NXR decreases may be due to the perturbation of gene expression patterns, i.e., the protein synthesis process.

Understandings of Inhibited Protein Synthesis Process. The process of protein synthesis is a complex process consisting of several steps, such as transcription, translation, and post-translational processing. These steps require the participation of ribosomes and many enzymatic and non-enzymatic proteins, such as RNA polymerase, necessary for transcription and translation factors and aminoacyl-tRNA (aa-tRNA) ligase responsible for the translation process. The protein synthesis of NOB was evaluated based on the DEPs involved in these steps.

Typically, transcription is thought to be the first step of protein synthesis, while coupled transcription-translation is considered a mark of protein synthesis in prokaryotic.[27,28] In transcription, mRNA is transcribed from DNA by RNA polymerase, which contains several essential subunits, including subunit alpha, beta, and omega in prokaryote.[29] However, metaproteomic analysis suggested that the expression of subunits alpha, beta, and omega were downregulated significantly in the treatment reactor (Figure 2B). RNA polymerase subunits alpha and beta catalyze the transcription process, while subunit omega promotes the assembly of RNA polymerase.[30] This indicates that the transcription process was adversely affected within NOB. Meanwhile, ribosomes bind concurrently to the mRNA with the aid of several ribosomal proteins, such as 30s ribosomal proteins S1 and S3.[31] However, 30s ribosomal proteins S1 and S3 derived from *N. defluvii* were detected to be downregulated by −4.231 $\log_2$(FC) and −3.358 $\log_2$(FC) in the treatment reactor (Figure 2B), respectively, signifying that the binding between mRNA and ribosome was also unfavorably influenced.

During transcription, ribosomes initiate the translation process at the same time. Generally, the translation process is divided into four steps: initiation, elongation, termination, and recycling, while each step is accomplished accurately based on the interaction between the relevant translation factors and the ribosome.[32] In addition, ribosomal proteins, such as 30s ribosomal protein S4, S5, and S12, and tRNA (e.g., aa-tRNA) are necessary for translation. The metaproteomic and metagenomic analyses were further applied to reveal the changes in the expression of these components and elucidate the effects on translation.

The initiation of translation in prokaryotes requires the coordinated activities of translation initiation factors (IF-1, IF-

https://doi.org/10.1021/acs.est.3c06002
Environ. Sci. Technol. XXXX, XXX, XXX−XXX

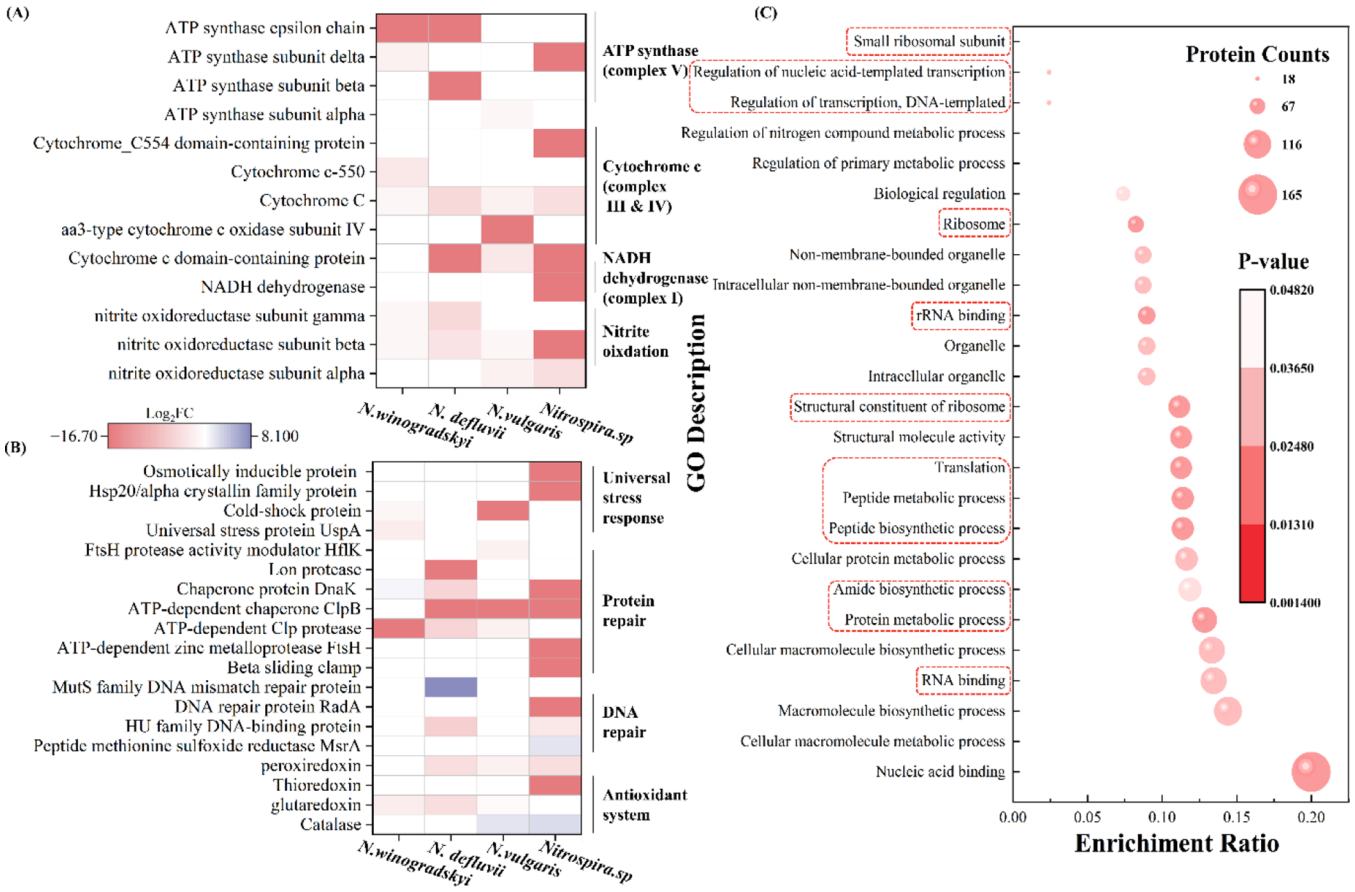

Figure 3. Heatmap showing the regulation of proteins related to (A) energy generation and (B) stress response system; white color indicates that FC does not satisfy the condition or p is greater than 0.05; (C) The bubble plot shows the results of the enrichment analysis based on GO (Gene Ontology); red boxes indicate the GO functions related to ribosome biogenesis or protein synthesis.

2, and IF-3)[33] (Figure 2A). Among them, IF-3 is responsible for separating the subunits from the ribosomes, which bind to the 30s ribosomal subunit and promote dissociation of the ribosome. After that, IF-2 facilitates binding the P site to the initiating tRNA,[34,35] and IF-1 is demonstrated to be essential for cells with crucial functions such as stimulating the activity of IF-2 and IF-3.[36] Statistical analyses showed that decreased expression levels of IF-1, IF-2, and IF-3 derived from several NOB populations were detected in the treatment reactor (Figure 2B), strongly indicating that translation initiation was adversely affected. Elongation is known as a highly conserved step catalyzed by elongation factors[37] following initiation. Elongation involves a sequential cycle including tRNA selection, peptidyl transfer, and translocation of tRNAs[38] (Figure 2A), and each process requires corresponding elongation factors described as the workhorses of protein synthesis.[39] The abundance of those translation elongation factors, including elongation factor Tu (ef-Tu), elongation factor G (ef-G), elongation factor P (ef-P), and elongation factor Ts (ef-TS), was detected to be remarkably down-regulated in the treatment reactor (Figure 2B). For instance, ef-Tu promotes aa-tRNA binding to the A-site of ribosomes and forms the EF-Tu-GTP complex,[37] which is further changed to GDP with the assistance of ef-Ts.[37] Severe decreases in the expression of both ef-Tu and ef-Ts for several NOB populations were seen in the treatment reactor (Figure 2B). In addition, ef-P was proven to stimulate efficient translation and peptide-bond synthesis, while ef-G catalyzed ribosomal translocation. The metaproteomic analyses showed that ef-P and ef-G were downregulated by −3.747 and −16.61 $\log_2$(FC) (Figure 2B), respectively. Overall, these elongation factors are essential for the translation elongation process in bacteria, and obviously, the elongation step of translation was seriously inhibited due to the restrained expression of elongation factors.

In addition, aa-tRNA ligase (synthetase) catalyzes the attachment of specific amino acids to appropriate tRNA, forming aa-tRNA, the substrate of the translation and protein synthesis.[40,41] For example, serine-tRNA ligase catalyzes the attachment of serine to tRNA (Ser), which is then delivered to the ribosome for protein synthesis. Statistical analyses suggested that the abundance of at least eight kinds of aa-tRNA ligase from several *Nitrospira* populations was significantly downregulated in the treatment reactor (Figure 2B). Additionally, the binding between aa-tRNA and ribosome seemed to be disturbed the same as mRNA due to decreased expression of relevant ribosomal proteins, such as 50s ribosomal protein L19 and 30s ribosomal protein S10[42] (Figure 2B). In brief, there is no doubt that the bioavailability of aa-tRNA within the NOB population was disrupted during NO_2^- accumulation, which may also contribute to inhibited protein synthesis.

It seems that the termination and recycling steps were not affected significantly, as only a DEP (ribosome-recycling factor (*N. defluvii*)) related to these steps was detected in this study. In addition, the regulation of proteins related to post-

https://doi.org/10.1021/acs.est.3c06002
Environ. Sci. Technol. XXXX, XXX, XXX−XXX

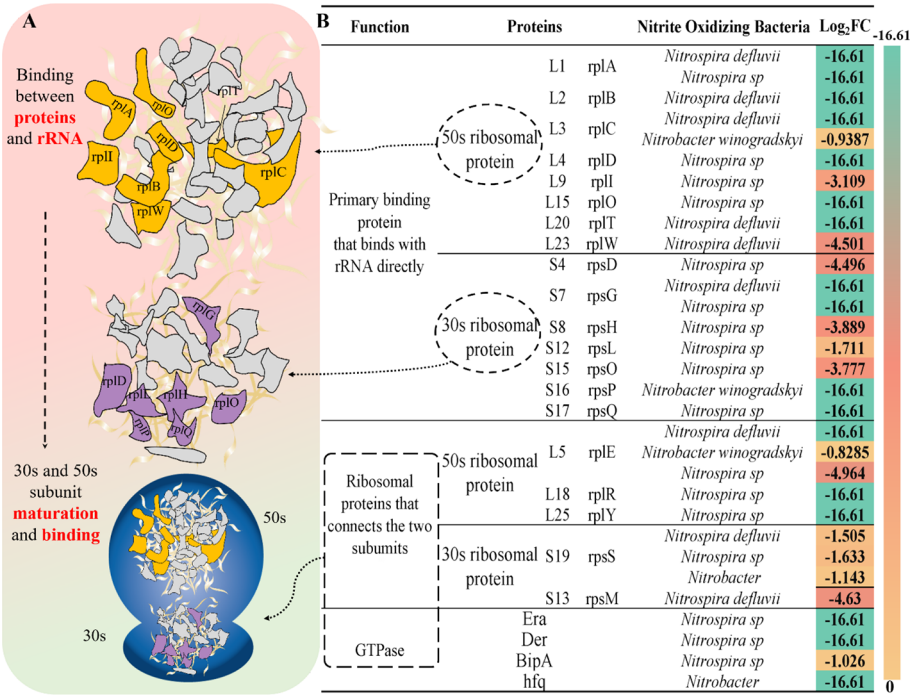

Figure 4. Schematic diagram showing various influences on the process of biogenesis of ribosome, and the overview of ribosomal proteins is modified from previous illustrations.[62] (B) The table shows some of the ribosomal proteins that are significantly downregulated under the combined interference, and the color scale is generated based on data of $\log_2$foldchange (treatment to control).

translational processing is shown in the Supporting Information. On the whole, this study not only proposed the influence on transcription, translation initiation, and elongation causing NOB inhibition and loss of nitrite oxidation capacity but also provided direct proof by identifying the decreased relevant enzymatic and nonenzymatic proteins (i.e., RNA polymerase, translation initiation factor, translation elongation factor and aminoacyl-tRNA ligase), as shown in Figure 2.

Revealing the Underlying Reasons for Inhibition on Protein Synthesis Processes. It should be noted that protein synthesis was affected by several factors. For instance, it has a huge demand for cellular resources, including cellular substances (amino acids)[43] and energy (ATP),[44] and environmental stress may also influence the rate of protein synthesis.[45] Most importantly, as described above, protein synthesis is highly dependent on the involvement of ribosomes as multiple steps are completed at the ribosome. Therefore, we further discussed the underlying mechanisms of the inhibited protein synthesis from these perspectives.

As mentioned above, protein synthesis is considered the most expensive macromolecular synthesis type in cells due to its high ATP consumption.[46,47] In addition, the substrates for protein synthesis are amino acids, which must be obtained through amino acid metabolism. Both ATP and amino acids are biosynthesized in the primary metabolism. In other words, protein synthesis is directly affected when primary metabolism is inhibited, and sufficient cellular resources are unavailable. Notably, we did detect significant downregulation of proteins related to energy generation and amino acid synthesis in several NOB species, such as NXR, ATP synthase, cysteine synthase, and threonine synthase (Figure 3A). However, despite these DEPs, enrichment analysis based on the Gene Ontology (GO) database showed that no significant difference was detected in energy production processes and amino acid metabolism between the reactors, which means that overall energy and amino acid generation were not significantly influenced. It may not be the major reason for inhibited protein synthesis.

In addition, the protein synthesis process is vulnerable to environmental stresses. For instance, when suffering DNA damage, cells may stop transcription until the DNA repair process is complete;[48] oxidative stress may influence protein synthesis by slowing or even completely stalling the translational elongation process.[49] To cope with environmental stress and maintain internal homeostasis, bacteria have evolved corresponding stress response systems such as DNA repair and antioxidant systems. However, we found that only a few oxidative stress enzymes and DNA repair proteins showed upregulation in the treatment reactor and most showed significant downregulation. For instance, catalase, known to be the key enzyme against ROS in bacteria,[50] was upregulated by 1.90 and 2.33 $\log_2$FC for *N. vulgaris* and *Nitrospira sp*, respectively (Figure 3B), while thioredoxin and glutaredoxin were detected to be downregulated in the treatment reactor. One possible explanation is that downregulation in stress response systems may lead to the inability to maintain internal homeostasis within the NOB, which further influences protein synthesis. However, a limited number of stress response system proteins were detected to be downregulated, while others did not significantly change expression. The GO enrichment analysis results also showed no significant change in the pathways related stress response system, such as GO:0006974 DNA damage response or GO:0098869 cellular oxidant detoxification (Figure 3C). Therefore, inhibited stress response systems may not be the primary reason as well.

Finally, the perturbation of the biogenesis of ribosomes within the NOB was believed to be the underlying reason for the adverse effect on protein synthesis. As mentioned above, many steps of protein synthesis depend on properly assembled and fully functional ribosomes including the entire translation

https://doi.org/10.1021/acs.est.3c06002
Environ. Sci. Technol. XXXX, XXX, XXX−XXX

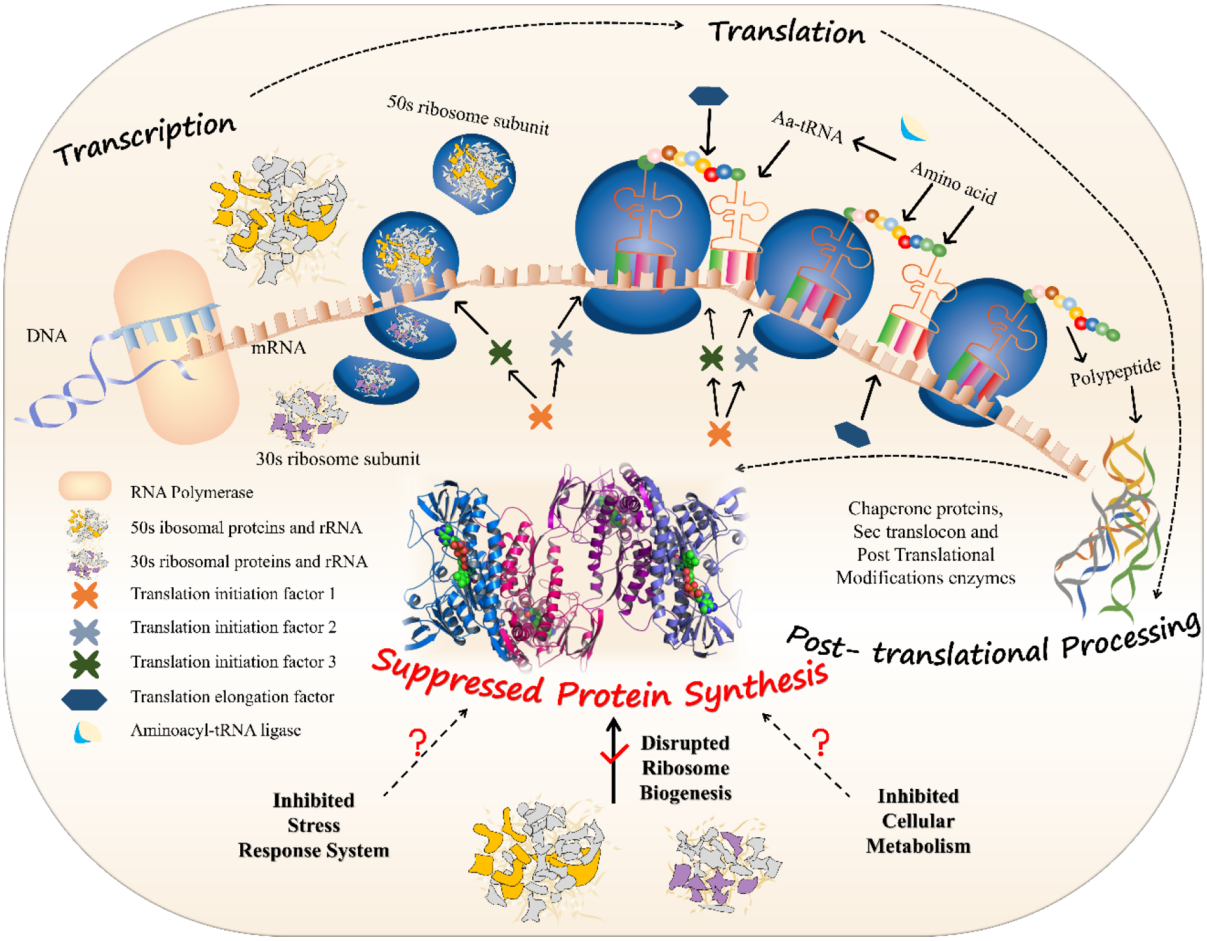

Figure 5. Overview model of the inhibition mechanisms of the combined interference on ribosome biogenesis and protein synthesis. The bold fonts represent downregulated proteins that are significant to the process: RNA polymerase, transcription; 50s and 30s ribosomal proteins, biogenesis of ribosome; translation initiation factor 1, stimulating activity of IF-2 and IF-3; translation initiation factor 2, binding the P site to the initiating tRNA; translation initiation factor 3, separating the subunits; translation elongation factor, translation elongation; aa-tRNA ligase, attachment of specific amino acids to appropriate tRNA.

process. In addition, the synthesis of RNA polymerase[51] and recruitment and activity of translation factors are regulated by the ribosomes.[52,53] Thus, the accurate and unambiguous process of ribosome biogenesis, including both binding between ribosomal proteins to rRNA (i.e., formation of subunits) and subunit-to-subunit binding, is of great importance for protein synthesis, even cellular activity.[54,55] More importantly, enrichment analysis based on the GO database showed that downregulated expressed proteins were significantly ($p < 0.05$) correlated with ribosomes and rRNA binding (Figure 3C). This indicates that the ribosome biogenesis in NOB may be severely disrupted, which may be one of the underlying mechanisms of protein synthesis.

Deregulation of Ribosome Biogenesis: Decrease of Ribosomal Proteins and GTPases. The prokaryotic ribosome consists of two subunits (i.e., 30s and 50s subunits), each containing different rRNA and dozens of ribosomal proteins. Ribosomal proteins play a vital role in ribosome biogenesis, exemplified by the essential housekeeping roles.[56] The 50s ribosomal proteins L1, L2, and 30s ribosomal proteins S4 and S7, described as universal ribosomal proteins,[57] connect with RNA in direct contact and complicate them, which is considered the first step in ribosomal subunit formation.[58,59] In this test, significant decreases in expression of these ribosomal proteins were observed in the treatment reactor (Figure 4B), which suggests the inability of the first step of ribosome biogenesis within the NOB. Moreover, 30s ribosomal protein S16 helps the assembly of the platform of the 30s subunit as another essential primary binding protein that binds to 16S rRNA directly. The 30s ribosomal protein S16 derived from *N. winogradskyi* was seen to be downregulated by $-16.61\log_2$FC in the treatment reactor. In addition, 50s ribosomal protein L5 is proven to play a pivotal role in the assembly of 50s ribosomal subunits, which is responsible for the binding between 50s and 30s subunits.[60] Correspondingly, 30s ribosomal protein S13 contacts 50s ribosomal protein L5 and contributes to connecting the two subunits.[61] In the present study, statistical analyses based on the multiomics showed that 50s ribosomal protein L5 (*N. defluvii*) was downregulated by -16.61 $\log_2$(FC) while 30s ribosomal protein S13 (*N. defluvii*) was downregulated by $-4.63\log_2$(FC) (Figure 4B). This suggests that not only the bindings between ribosomal proteins and rRNA but also the consequent bindings between ribosome subunits were inhibited.

Some other evidence supports this speculation, as well. For example, GTPases regulate numerous cellular processes and play a key role in ribosome biogenesis in *E. coli*. Specifically, GTPases Era and RsgA are related to the maturation of the 30s ribosomal subunits in *Escherichia coli*, while GTPases Era and

https://doi.org/10.1021/acs.est.3c06002
Environ. Sci. Technol. XXXX, XXX, XXX−XXX

Der (double Era-like GTPase) are relevant to the assembly of the 50s ribosomal subunits.[63−66] The metaproteomic analysis showed that the abundance of GTPases such as Era and Der in NOB was significantly downregulated with a log_2FC of −16.61 (Figure 4B). In addition, bipA, functioning in the 50s subunit biogenesis,[67] decreased with a Log_2FC of −1.026. In conclusion, we proposed that decreases in ribosomal protein and GTPase expression perturb the biogenesis of ribosomes, which is a primary cellular process for maintaining ribosome homeostasis and gene expression. Given the importance of ribosomes, the adverse influence on the biogenesis of ribosomes should be the major cause of inhibited protein synthesis and NOB inhibition, even inactivation, which ultimately leads to the loss of NO_2^- oxidation capacity.

Based on these findings, we proposed an overview to diagrammatically show the underlying mechanisms of NOB inhibition causing NO_2^- accumulation (Figure 5). First, in this study, the abundance of NXR was significantly reduced in the treatment reactor, which means a loss of NO_2^-oxidation capacity and directly results in accumulation of NO_2^-. Since NXR is essentially an enzymatic protein, the possible explanation is that the protein synthesis process was inhibited, as evidenced by the downregulation of RNA polymerase and translation factors, which play vital roles in the transcription, translation initiation, and elongation. Further investigations revealed that ribosome biogenesis was significantly affected in NOB due to decreased levels of ribosomal proteins and GTPases. In particular, several primary binding proteins responsible for formation of subunits, such as 50s ribosomal proteins L1 and L2 and 30s ribosomal proteins S4 and S7, were downregulated significantly, which means that the first step of ribosome biogenesis was disturbed. In addition, metaproteomic analysis showed that primary metabolism (energy production and amino acid synthesis, etc.) and stress systems (oxidative stress, DNA repair, etc.) were also adversely affected within NOB, which would contribute to the inhibited protein synthesis as well. Knowing the critical role of ribosomes in protein synthesis, the disruption of ribosome biogenesis was believed to be the underlying reason for inhibited protein synthesis, which results in NOB suppression and eventually leads to NO_2^- accumulation.

Environmental Implications. Several significant implications are proposed with the following considerations. First, achieving the paradigm shift in the operation of WWTPs to establish a circular economy, i.e., from pollutant removal to resource recovery, is of practical significance in the 21st century. Partial nitrification/anammox (PN/A), also known as mainstream deammonification, is widely considered the most promising method with the major challenge of achieving stable NOB suppression. Our study provides novel and profound insights into achieving stable NOB suppression from a molecular perspective. High metabolic flexibility and physiological diversity of NOB have been proposed as new hurdles for stable PN, which resulted in a predestined inability to suppress all NOB species from current perspectives. It is suggested that stable suppression of NOB could be established by disrupting ribosome biogenesis, thereby affecting protein synthesis, which is generally a conserved but susceptible cellular process with significant correlations to cell proliferation.[54] Due to the conservatism, disrupting ribosome biogenesis is an effective strategy for inhibiting all NOB species. It would not fail due to physiological and phylogenetic redundancy (e.g., diversity of metabolism and stress response systems) among NOB species when the NOB population shifts. The potential for application of physical and chemical factors (e.g., ultrasound, cold stress, radiation, and biocides) that can affect ribosome biogenesis should be comprehensively evaluated to find the most suitable strategy for stable NOB suppression. In addition, when extrapolated to full-scale WWTPs, it is also necessary to consider whether these strategies would inhibit other functional microorganisms in the overall sludge microbial community, such as AOB and denitrifiers, thus affecting the removal of other pollutants.

Second, although denitrifiers and anammox bacteria are NO_2^- consumers, the conversion of NO_2^- to NO_3^- can only be achieved by NOB. According to Zhang et al.,[68] NO_2^- and NO_3^- concentrations are the key factors driving N cycle in eutrophic lakes, which means that NO_2^- may affect the transformation of nitrogen compounds in sediments. Of importance to note is that FA concentration (5−6 mg NH_3−N/L) in eutrophic lake sediment reached the NOB inhibition level,[17,68] which would lead to NO_2^- accumulation. High concentrations of NO_2^- are strongly toxic to aquatic organisms and microorganisms, making fragile eutrophic ecosystems even more vulnerable. Moreover, the accumulation of NO_2^- tends to enhance the denitrification of AOB, thus increasing N_2O emission in eutrophic environments,[69] which are already hotspots for N_2O emissions.[70,71] In addition, extreme conditions due to anthropogenic activities, such as wastewater shock containing high NH_4^+-N and concentrated discharge of ribosome-targeted antibiotics, may induce direct damage to the ribosomes of NOB, resulting in irreversible loss of NO_2^- oxidation. Efforts should be made to maintain the activity of ribosome biogenesis and protein synthesis within the NOB to avoid NO_2^- accumulation under these conditions.

In conclusion, our study provided the first experimental evidence that disrupted ribosome biogenesis and protein synthesis in NOB was the underlying mechanism for its inability to remain active and loss of the NO_2^- oxidation capacity. The limitation of our study was that we evaluated only the NO_2^- accumulation established by sludge treatment using FA, but it was an advantageous supplement to the underlying mechanisms of NO_2^- accumulation at least. Whether other treatment measures or environmental perturbations affect NOB in the same way deserves more investigations in the future, and our study provides a paradigm. In addition, the reasons for the decrease in ribosomal proteins and GTPases remain unknown. Previous studies on rats and human cells demonstrated that ammonia impairs ribosome biogenesis and protein synthesis by causing degradation of β-catenin, a transcriptional activator of ribosomal biogenesis regulator.[72] Nevertheless, no significant change in expression of the ribosomal biogenesis regulator was detected in this test. More studies based on molecular and cellular biology are needed for further investigations of the instability of the NOB ribosome biogenesis. Filling these knowledge gaps will not only improve our understanding of the nitrogen biogeochemical cycle but also advance the development of engineering optimization strategies.

■ ASSOCIATED CONTENT

Supporting Information

The Supporting Information is available free of charge at https://pubs.acs.org/doi/10.1021/acs.est.3c06002.

https://doi.org/10.1021/acs.est.3c06002
Environ. Sci. Technol. XXXX, XXX, XXX−XXX

(Table S1) Detailed information for all DEPs discussed in this study (XLSX)

Materials and methods of the batch test, DNA extraction, protein extraction, protein dissolution, sodium dodecyl sulfate-polyacrylamide gel electrophoresis (SDS-PAGE) assay, high-performance liquid chromatography (HPLC) assay, and mass spectrometry analysis; discussion of effect on post-translational processing; statistics of the metagenomic sequences (Table S1); determined protein concentrations of samples by the bicinchoninic acid method (Table S2); parameters showing main reactor performance at the end of the experiment (Table S3); sample concentrations determined by the BCA method (Table S4); sodium dodecyl sulfate-polyacrylamide gel electrophoresis picture of samples for protein profile 125 quality check (Figure S1); nitrogen compounds in the effluent of the control reactor (Figure S2); top 10 of the nitrifier species in the reactor based on the relative abundance-(Figure S3); overview of the top 50 genus of the microbial community, and the color scale is generated based on data of relative abundance (Figure S4); changes in concentration of nitrogen compounds over a typical operating cycle at the end of baseline stage (day 100−110) (Figure S5); changes in concentration of nitrogen compounds over a typical operating cycle at the end of baseline stage (day 200−210) (Figure S6) (PDF)

AUTHOR INFORMATION

Corresponding Author

Dongbo Wang − *College of Environmental Science and Engineering and Key Laboratory of Environmental Biology and Pollution Control (Ministry of Education), Hunan University, Changsha 410082, PR China*; Email: dongbowang@hnu.edu.cn

Authors

Weiping Xiong − *College of Environmental Science and Engineering and Key Laboratory of Environmental Biology and Pollution Control (Ministry of Education), Hunan University, Changsha 410082, PR China*; orcid.org/0000-0001-8022-0115

Yuhang Ye − *College of Environmental Science and Engineering and Key Laboratory of Environmental Biology and Pollution Control (Ministry of Education), Hunan University, Changsha 410082, PR China*

Dandan He − *College of Environmental Science and Engineering and Key Laboratory of Environmental Biology and Pollution Control (Ministry of Education), Hunan University, Changsha 410082, PR China*

Siying He − *College of Environmental Science and Engineering and Key Laboratory of Environmental Biology and Pollution Control (Ministry of Education), Hunan University, Changsha 410082, PR China*

Yinping Xiang − *College of Environmental Science and Engineering and Key Laboratory of Environmental Biology and Pollution Control (Ministry of Education), Hunan University, Changsha 410082, PR China*

Jun Xiao − *College of Environmental Science and Engineering and Key Laboratory of Environmental Biology and Pollution Control (Ministry of Education), Hunan University, Changsha 410082, PR China*

Wenyi Feng − *College of Environmental Science and Engineering and Key Laboratory of Environmental Biology and Pollution Control (Ministry of Education), Hunan University, Changsha 410082, PR China*

Mengru Wu − *College of Environmental Science and Engineering and Key Laboratory of Environmental Biology and Pollution Control (Ministry of Education), Hunan University, Changsha 410082, PR China*

Zhaohui Yang − *College of Environmental Science and Engineering and Key Laboratory of Environmental Biology and Pollution Control (Ministry of Education), Hunan University, Changsha 410082, PR China*

Complete contact information is available at: https://pubs.acs.org/10.1021/acs.est.3c06002

Notes

The authors declare no competing financial interest.

ACKNOWLEDGMENTS

The study was financially supported by the National Youth Foundation of China (52000064), the Natural Science Foundation of Hunan Province (2023JJ0013), the Science and Technology Innovation Program of Hunan Province (2021RC4024), Technology Innovation Program of China Postdoctoral Science Foundation (2022M721089), and Xiaohe Sci-Tech Talents Special Funding under Hunan Provincial Sci-Tech Talents Sponsorship Program (2023TJ-X21).

REFERENCES

(1) Xia, W.; Zhang, C.; Zeng, X.; Feng, Y.; Weng, J.; Lin, X.; Zhu, J.; Xiong, Z.; Xu, J.; Cai, Z.; Jia, Z. Autotrophic growth of nitrifying community in an agricultural soil. *ISME J.* **2011**, *5* (7), 1226−1236.

(2) Pérez, J.; Buchanan, A.; Mellbye, B.; Ferrell, R.; Chang, J. H.; Chaplen, F.; Bottomley, P. J.; Arp, D. J.; Sayavedra-Soto, L. A. Interactions of Nitrosomonas europaea and Nitrobacter winogradskyi grown in co-culture. *Arch. Microbiol.* **2015**, *197* (1), 79−89.

(3) Casciotti, K. L.; Buchwald, C. Insights on the marine microbial nitrogen cycle from isotopic approaches to nitrification. *Front. Microbiol.* **2012**, *3*, 356 DOI: 10.3389/fmicb.2012.00356.

(4) Schaefer, S. C.; Hollibaugh, J. T. Temperature Decouples Ammonium and Nitrite Oxidation in Coastal Waters. *Environ. Sci. Technol.* **2017**, *51* (6), 3157−3164.

(5) Jetten, M. S. M.; Horn, S. J.; van Loosdrecht, M. C. M. Towards a more sustainable municipal wastewater treatment system. *Water Sci. Technol.* **1997**, *35* (9), 171−180.

(6) Wang, L.; Gu, W.; Liu, Y.; Liang, P.; Zhang, X.; Huang, X. Challenges, solutions and prospects of mainstream anammox-based process for municipal wastewater treatment. *Sci. Total Environ.* **2022**, *820*, No. 153351.

(7) Graham, D. W.; Knapp, C. W.; Van Vleck, E. S.; Bloor, K.; Lane, T. B.; Graham, C. E. Experimental demonstration of chaotic instability in biological nitrification. *ISME J.* **2007**, *1* (5), 385−393.

(8) Philips, S.; Laanbroek, H. J.; Verstraete, W. Origin, causes and effects of increased nitrite concentrations in aquatic environments. *Rev. Environ. Sci. Biotechnol.* **2002**, *1* (2), 115−141.

(9) Kim, D.-J.; Lee, D.-I.; Keller, J. Effect of temperature and free ammonia on nitrification and nitrite accumulation in landfill leachate and analysis of its nitrifying bacterial community by FISH. *Bioresour. Technol.* **2006**, *97* (3), 459−468.

(10) Vadivelu, V. M.; Keller, J.; Yuan, Z. Effect of free ammonia on the respiration and growth processes of an enriched Nitrobacter culture. *Water Res.* **2007**, *41* (4), 826−834.

(11) Sun, H.; Jiang, T.; Zhang, F.; Zhang, P.; Zhang, H.; Yang, H.; Lu, J.; Ge, S.; Ma, B.; Ding, J.; Zhang, W. Understanding the effect of free ammonia on microbial nitrification mechanisms in suspended activated sludge bioreactors. *Environ. Res.* **2021**, *200*, No. 111737.

(12) Giguere, A. T.; Taylor, A. E.; Suwa, Y.; Myrold, D. D.; Bottomley, P. J. Uncoupling of ammonia oxidation from nitrite oxidation: Impact upon nitrous oxide production in non-cropped Oregon soils. *Soil Biol. Biochem.* **2017**, *104*, 30−38.
(13) Kocour Kroupová, H.; Valentová, O.; Svobodová, Z.; Šauer, P.; Máchová, J. Toxic effects of nitrite on freshwater organisms: a review. *Rev. Aquacult.* **2018**, *10* (3), 525−542.
(14) Schmeing, T. M.; Voorhees, R. M.; Kelley, A. C.; Gao, Y. G.; Murphy, F. V.; Weir, J. R.; Ramakrishnan, V. The Crystal Structure of the Ribosome Bound to EF-Tu and Aminoacyl-tRNA. *Science* **2009**, *326* (5953), 688−694.
(15) Webster, M. W.; Takacs, M.; Zhu, C.; Vidmar, V.; Eduljee, A.; Abdelkareem, M.; Weixlbaumer, A. Structural basis of transcription-translation coupling and collision in bacteria. *Science* **2020**, *369* (6509), 1355.
(16) Gamalinda, M.; Woolford, J. L., Jr. Paradigms of ribosome synthesis: Lessons learned from ribosomal proteins. *Translation* **2015**, *3* (1), e975018.
(17) Liu, Y.; Ngo, H. H.; Guo, W.; Peng, L.; Wang, D.; Ni, B. The roles of free ammonia (FA) in biological wastewater treatment processes: A review. *Environ. Int.* **2019**, *123*, 10−19.
(18) Fu, Q.; Long, S.; Xu, Y.; Wang, Y.; Yang, B.; He, D.; Li, X.; Liu, X.; Lu, Q.; Wang, D. Revealing an unrecognized role of free ammonia in sulfur transformation during sludge anaerobic treatment. *J. Hazard. Mater.* **2023**, *452*, 131305.
(19) Wang, D.; Pan, C.; Chen, L.; He, D.; Yuan, L.; Li, Y.; Wu, Y. Positive feedback on dewaterability of waste-activated sludge by the conditioning process of Fe(II) catalyzing urea hydrogen peroxide. *Water Res.* **2022**, *225*, No. 119195, DOI: 10.1016/j.watres.2022.119195.
(20) Wang, Q.; Duan, H.; Wei, W.; Ni, B. J.; Laloo, A.; Yuan, Z. Achieving Stable Mainstream Nitrogen Removal via the Nitrite Pathway by Sludge Treatment Using Free Ammonia. *Environ. Sci. Technol.* **2017**, *51* (17), 9800−9807.
(21) Bian, Y.; Wang, D.; Liu, X.; Yang, Q.; Liu, Y.; Wang, Q.; Ni, B.-J.; Li, H.; Zhang, Y. The fate and impact of TCC in nitrifying cultures. *Water Res.* **2020**, *178*, No. 115851, DOI: 10.1016/j.watres.2020.115851.
(22) Li, D.; Luo, R.; Liu, C.-M.; Leung, C.-M.; Ting, H.-F.; Sadakane, K.; Yamashita, H.; Lam, T.-W. MEGAHIT v1.0: A fast and scalable metagenome assembler driven by advanced methodologies and community practices. *Methods* **2016**, *102*, 3−11.
(23) Noguchi, H.; Park, J.; Takagi, T. MetaGene: prokaryotic gene finding from environmental genome shotgun sequences. *Nucleic Acids Res.* **2006**, *34* (19), 5623−5630.
(24) Fu, L.; Niu, B.; Zhu, Z.; Wu, S.; Li, W. CD-HIT: accelerated for clustering the next-generation sequencing data. *Bioinformatics* **2012**, *28* (23), 3150−3152.
(25) Li, R.; Li, Y.; Kristiansen, K.; Wang, J. SOAP: short oligonucleotide alignment program. *Bioinformatics* **2008**, *24* (5), 713−714.
(26) Daims, H.; Lücker, S.; Wagner, M. A New Perspective on Microbes Formerly Known as Nitrite-Oxidizing Bacteria. *Trends Microbiol.* **2016**, *24* (9), 699−712.
(27) Irastortza-Olaziregi, M.; Amster-Choder, O. Coupled Transcription-Translation in Prokaryotes: An Old Couple With New Surprises. *Front. Microbiol.* **2021**, *11*, No. 624830.
(28) Fan, H.; Conn, A. B.; Williams, P. B.; Diggs, S.; Hahm, J.; Gamper, H. B., Jr; Hou, Y. M.; O'Leary, S. E.; Wang, Y.; Blaha, G. M. Transcription-translation coupling: direct interactions of RNA polymerase with ribosomes and ribosomal subunits. *Nucleic Acids Res.* **2017**, *45* (19), 11043−11055.
(29) Werner, F. Structure and function of archaeal RNA polymerases. *Mol. Microbiol.* **2007**, *65* (6), 1395−1404.
(30) Gross, C. A.; Chan, C. L.; Lonetto, M. A. A structure/function analysis of Escherichia coli RNA polymerase. *Philos. Trans. R. Soc. London, Ser. B: Biol. Sci.* **1996**, *351* (1339), 475−482.
(31) Lücker, S.; Wagner, M.; Maixner, F.; Pelletier, E.; Koch, H.; Vacherie, B.; Rattei, T.; Damsté, J. S. S.; Spieck, E.; Le Paslier, D.; Daims, H. A Nitrospira metagenome illuminates the physiology and evolution of globally important nitrite-oxidizing bacteria. *Proc. Natl. Acad. Sci. U.S.A.* **2010**, *107* (30), 13479−13484.
(32) Seely, S. M.; Gagnon, M. G. Mechanisms of ribosome recycling in bacteria and mitochondria: a structural perspective. *RNA Biol.* **2022**, *19* (1), 662−677.
(33) Choi, S. K.; Olsen, D. S.; Roll-Mecak, A.; Martung, A.; Remo, K. L.; Burley, S. K.; Hinnebusch, A. G.; Dever, T. E. Physical and functional interaction between the eukaryotic orthologs of prokaryotic translation initiation factors IF1 and IF2. *Mol. Cell. Biol.* **2000**, *20* (19), 7183−7191.
(34) Choi, S. K.; Lee, J. H.; Zoll, W. L.; Merrick, W. C.; Dever, T. E. Promotion of met-tRNAiMet binding to ribosomes by yIF2, a bacterial IF2 homolog in yeast. *Science* **1998**, *280* (5370), 1757−1760.
(35) Lee, J. H.; Choi, S. K.; Roll-Mecak, A.; Burley, S. K.; Dever, T. E. Universal conservation in translation initiation revealed by human and archaeal homologs of bacterial translation initiation factor IF2. *Proc. Natl. Acad. Sci. U.S.A.* **1999**, *96* (8), 4342−4347.
(36) Laursen, B. S.; Sørensen, H. P.; Mortensen, K. K.; Sperling-Petersen, H. U. Initiation of protein synthesis in bacteria. *Microbiol. Mol. Biol. Rev.* **2005**, *69* (1), 101−123.
(37) Zhang, L.; Wang, Y.; Dai, H.; Zhou, J. Structural and functional studies revealed key mechanisms underlying elongation step of protein translation. *Acta Biochim. Biophys. Sin.* **2020**, *52* (7), 749−756.
(38) Prabhakar, A.; Choi, J.; Wang, J.; Petrov, A.; Puglisi, J. D. Dynamic basis of fidelity and speed in translation: Coordinated multistep mechanisms of elongation and termination. *Protein Sci.* **2017**, *26* (7), 1352−1362.
(39) Andersen, G. R.; Nissen, P.; Nyborg, J. Elongation factors in protein biosynthesis. *Trends Biochem. Sci.* **2003**, *28* (8), 434−441.
(40) Ibba, M.; Söll, D. Aminoacyl-tRNA synthesis. *Annu. Rev. Biochem.* **2000**, *69* (1), 617−650.
(41) Gao, Y. G.; Selmer, M.; Dunham, C. M.; Weixlbaumer, A.; Kelley, A. C.; Ramakrishnan, V. The structure of the ribosome with elongation factor G trapped in the posttranslocational state. *Science* **2009**, *326* (5953), 694−699.
(42) Parks, D. H.; Chuvochina, M.; Waite, D. W.; Rinke, C.; Skarshewski, A.; Chaumeil, P. A.; Hugenholtz, P. A standardized bacterial taxonomy based on genome phylogeny substantially revises the tree of life. *Nat. Biotechnol.* **2018**, *36* (10), 996−1004.
(43) Yan, L.; Lamb, R. F. Amino acid sensing and regulation of mTORC1. *Semin. Cell Dev. Biol.* **2012**, *23* (6), 621−625.
(44) Pontes, M. H.; Sevostyanova, A.; Groisman, E. A. When Too Much ATP Is Bad for Protein Synthesis. *J. Mol. Biol.* **2015**, *427* (16), 2586−2594.
(45) Ríus, A. G. Invited Review: Adaptations of protein and amino acid metabolism to heat stress in dairy cows and other livestock species. *Appl. Anim. Sci.* **2019**, *35* (1), 39−48.
(46) Söllinger, A.; Séneca, J.; Borg Dahl, M.; Motleleng, L. L.; Prommer, J.; Verbruggen, E.; Sigurdsson, B. D.; Janssens, I.; Peñuelas, J.; Urich, T.; Richter, A.; Tveit, A. T. Down-regulation of the bacterial protein biosynthesis machinery in response to weeks, years, and decades of soil warming. *Sci. Adv.* **2022**, *8* (12), eabm3230.
(47) Buttgereit, F.; Brand, M. D. A hierarchy of ATP-consuming processes in mammalian cells. *Biochem. J.* **1995**, *312* (1), 163−167.
(48) Jain, S.; Gupta, R.; Sen, R. Rho-dependent transcription termination in bacteria recycles RNA polymerases stalled at DNA lesions. *Nat. Commun.* **2019**, *10* (1), 1207.
(49) Zhu, M.; Dai, X. Bacterial stress defense: the crucial role of ribosome speed. *Cell. Mol. Life Sci.* **2020**, *77* (5), 853−858.
(50) Semchyshyn, H. M.; Lushchak, V. I. Oxidative stress and control of catalase activity in Escherichia coli. *Ukr. Biokhim. Zh. (1999)* **2004**, *76* (2), 31−42.
(51) Ishihama, A.; Fukuda, R. Autogenous and post-transcriptional regulation of RNA polymerase synthesis. *Mol. Cell. Biochem.* **1980**, *31* (3), 177−196.
(52) Wang, L.; Yang, F.; Zhang, D.; Chen, Z.; Xu, R.-M.; Nierhaus, K. H.; Gong, W.; Qin, Y. A conserved proline switch on the ribosome

https://doi.org/10.1021/acs.est.3c06002
Environ. Sci. Technol. XXXX, XXX, XXX−XXX

facilitates the recruitment and binding of trGTPases. *Nat. Struct. Mol. Biol.* **2012**, *19* (4), 403−410.
(53) Zhang, D.; Liu, G.; Xue, J.; Lou, J.; Nierhaus, K. H.; Gong, W.; Qin, Y. Common chaperone activity in the G-domain of trGTPase protects L11-L12 interaction on the ribosome. *Nucleic Acids Res.* **2012**, *40* (21), 10851−10865.
(54) Yu, G.; Zhao, Y.; Li, H. The multistructural forms of box C/D ribonucleoprotein particles. *RNA* **2018**, *24* (12), 1625−1633.
(55) Davis, J. H.; Tan, Y. Z.; Carragher, B.; Potter, C. S.; Lyumkis, D.; Williamson, J. R. Modular Assembly of the Bacterial Large Ribosomal Subunit. *Cell* **2016**, *167* (6), 1610−1622.
(56) Zhou, X.; Liao, W. J.; Liao, J. M.; Liao, P.; Lu, H. Ribosomal proteins: functions beyond the ribosome. *J. Mol. Cell Biol.* **2015**, *7* (2), 92−104.
(57) Korobeinikova, A. V.; Garber, M. B.; Gongadze, G. M. Ribosomal proteins: structure, function, and evolution. *Biochemistry (Moscow)* **2012**, *77* (6), 562−574.
(58) Held, W. A.; Nomura, M. Rate determining step in the reconstitution of Escherichia coli 30S ribosomal subunits. *Biochemistry* **1973**, *12* (17), 3273−3281.
(59) Röhl, R.; Nierhaus, K. H. Assembly map of the large subunit (50S) of Escherichia coli ribosomes. *Proc. Natl. Acad. Sci. U.S.A.* **1982**, *79* (3), 729−733.
(60) Korepanov, A. P.; Korobeinikova, A. V.; Shestakov, S. A.; Garber, M. B.; Gongadze, G. M. Protein L5 is crucial for in vivo assembly of the bacterial 50S ribosomal subunit central protuberance. *Nucleic Acids Res.* **2012**, *40* (18), 9153−9159.
(61) Trylska, J.; McCammon, J. A.; Brooks, C. L. Exploring assembly energetics of the 30S ribosomal subunit using an implicit solvent approach. *J. Am. Chem. Soc.* **2005**, *127* (31), 11125−11133.
(62) Feliciano, J. R.; Seixas, A. M. M.; Pita, T.; Leitão, J. H. Comparative Genomics and Evolutionary Analysis of RNA-Binding Proteins of Burkholderia cenocepacia J2315 and Other Members of the B. cepacia Complex. *Front. Mol. Biosci.* **2020**, *11* (2), 231.
(63) Karbstein, K. Role of GTPases in ribosome assembly. *Biopolymers* **2007**, *87* (1), 1−11.
(64) Hwang, J.; Inouye, M. The tandem GTPase, Der, is essential for the biogenesis of 50S ribosomal subunits in Escherichia coli. *Mol. Microbiol.* **2006**, *61* (6), 1660−1672.
(65) Jiang, M.; Datta, K.; Walker, A.; Strahler, J.; Bagamasbad, P.; Andrews, P. C.; Maddock, J. R. The Escherichia coli GTPase CgtAE is involved in late steps of large ribosome assembly. *J. Bacteriol.* **2006**, *188* (19), 6757−6770.
(66) Choi, E.; Kang, N.; Jeon, Y.; Pai, H. S.; Kim, S. G.; Hwang, J. Heterologous Expression of Der Homologs in an Escherichia coli der Mutant and Their Functional Complementation. *J. Bacteriol.* **2016**, *198* (17), 2284−2296.
(67) Gibbs, M. R.; Fredrick, K. Roles of elusive translational GTPases come to light and inform on the process of ribosome biogenesis in bacteria. *Mol. Microbiol.* **2018**, *107* (4), 445−454.
(68) Zhang, D.; Li, M.; Yang, Y.; Yu, H.; Xiao, F.; Mao, C.; Huang, J.; Yu, Y.; Wang, Y.; Wu, B.; Wang, C.; Shu, L.; He, Z.; Yan, Q. Nitrite and nitrate reduction drive sediment microbial nitrogen cycling in a eutrophic lake. *Water Res.* **2022**, *220*, No. 118637.
(69) Chen, X.; Yuan, Z.; Ni, B.-J. Nitrite accumulation inside sludge flocs significantly influencing nitrous oxide production by ammonium-oxidizing bacteria. *Water Res.* **2018**, *143*, 99−108.
(70) Zhou, Y.; Xu, X.; Song, K.; Yeerken, S.; Deng, M.; Li, L.; Riya, S.; Wang, Q.; Terada, A. Nonlinear pattern and algal dual-impact in N2O emission with increasing trophic levels in shallow lakes. *Water Res.* **2021**, *203*, No. 117489, DOI: 10.1016/j.watres.2021.117489.
(71) Wang, Y.; Peng, Y.; Lv, C.; Xu, X.; Meng, H.; Zhou, Y.; Wang, G.; Lu, Y. Quantitative discrimination of algae multi-impacts on N2O emissions in eutrophic lakes: Implications for N2O budgets and mitigation. *Water Res.* **2023**, *235*, No. 119857, DOI: 10.1016/j.watres.2023.119857.
(72) Davuluri, G.; Giusto, M.; Chandel, R.; Welch, N.; Alsabbagh, K.; Kant, S.; Kumar, A.; Kim, A.; Gangadhariah, M.; Ghosh, P. K.; Tran, U.; Krajcik, D. M.; Vasu, K.; DiDonato, A. J.; DiDonato, J. A.; Willard, B.; Monga, S. P.; Wang, Y.; Fox, P. L.; Stark, G. R.; Wessely, O.; Esser, K. A.; Dasarathy, S. Impaired Ribosomal Biogenesis by Noncanonical Degradation of β-Catenin during Hyperammonemia. *Mol. Cell. Biol.* **2019**, *39* (16), e00451-18 DOI: 10.1128/mcb.00451-18.

https://doi.org/10.1021/acs.est.3c06002
Environ. Sci. Technol. XXXX, XXX, XXX−XXX